frontiers in
NEUROENERGETICS

ORIGINAL RESEARCH ARTICLE
published: 30 July 2010
doi: 10.3389/fnene.2010.00019

The biological effect of contralateral forepaw stimulation in rat focal cerebral ischemia: a multispectral optical imaging study

*Janos Luckl[1†], Wesley Baker[2], Zheng-Hui Sun[1], Turgut Durduran[2‡], Arjun G. Yodh[2] and Joel H. Greenberg[1]**

[1] Department of Neurology, University of Pennsylvania, Philadelphia, PA, USA
[2] Department of Physics and Astronomy, University of Pennsylvania, Philadelphia, PA, USA

Edited by:
David Boas, Massachusetts General Hospital, USA; Massachusetts Institute of Technology, USA; Harvard Medical School, USA

Reviewed by:
Ilknur Ay, Massachusetts General Hospital, USA
Bruno Weber, University of Zurich, Switzerland

****Correspondence:***
Joel H. Greenberg, Cerebrovascular Research Center, Department of Neurology, University of Pennsylvania, 415 Stemmler Hall, 3450 Hamilton Walk, Philadelphia, PA 19104-6063, USA.
e-mail: joel@upenn.edu
Present address:
[†]Department of Experimental Neurology, Charite-Universitatsmedizin Berlin, Berlin, Germany.
[‡] ICFO- Institut de Ciències Fotòniques, Mediterranean Technology Park, 08860 Castelldefels (Barcelona), Spain.

Our group has already published the possible neuroprotective effect of contralateral forepaw stimulation in temporary focal ischemia in a study. However, the background is still unclear. In the present study we investigated the possible mechanism by monitoring focal ischemia with multispectral [laser speckle, imaging of intrinsic signals (OIS)] imaging. Sprague–Dawley rats were prepared using 1.2% isoflurane anesthesia. The middle cerebral artery was occluded by photothrombosis (4 mW) and the common carotid artery was ligated permanently. Physiological variables were constantly monitored during the experiment. A 6 × 6 mm area centered 3 mm posterior and 4 mm lateral to Bregma was thinned for laser speckle and OIS imaging. Nine circular regions of interests (0.3 mm in diameter) were evenly spaced on the speckle contrast image for the analysis of peri-infarct flow transients, blood flow, and metabolic changes. Both the sham (n = 7) and forepaw-stimulated animals (n = 7) underwent neurological examinations 24 h after ischemia at which point all animals were sacrificed and the infarct size was determined by triphenyltetrazolium chloride. The physiological variables were in normal range and the experimental protocol did not cause significant differences between groups. Both the neurological scores (sham: 3.6 ± 1.7, stimulated: 4.3 ± 1.4) and the infarct volume (sham: 124 ± 39 mm^3, stimulated: 147 ± 47 mm^3) did not show significant differences between groups. The forepaw stimulation did not increase the intra-ischemic flow neither over the penumbral or the peri-ischemic area. However, the hemoglobin transients related metabolic load ($CMRO_2$) was significantly lower ($p < 0.001$) while the averaged number of hyperemic flow transients were significantly (p = 0.013) higher in the forepaw (sham: 3.5 ± 2.2, stimulated: 7.0 ± 2.3) stimulated animals.

Keywords: optical imaging, focal cerebral ischemia, forepaw stimulation, middle cerebral artery occlusion, photothrombosis, speckle contrast, OIS, flow transients

INTRODUCTION

Although many compounds have been investigated in cerebral ischemia, none have so far proven clinically useful in humans. Therefore, there is an intense interest in developing novel, non-pharmacological therapies. Techniques, such as the production of hypothermia (Yanamoto et al., 1999) and hyperoxemia (Shin et al., 2006), have been investigated intensively, but it remains to be seen how they transfer from laboratory to bedside. The use of electrical/magnetic stimulation represent a new direction in the treatment of various diseases of the central nervous system (CNS). Neuromuscular electrical stimulation (Chae et al., 2008), repetitive transcranial magnetic stimulation (rTMS) (Williams et al., 2009), and epidural cortical stimulation (Brown et al., 2006) all seem to be promising in the rehabilitation (improving motor function and pain) of stroke patients. The successful application of post-stroke stimulation raises the question as to whether patients could benefit from stimulation during acute cerebral ischemia. We previously showed that contralateral forepaw stimulation can reduce tissue injury if administered during temporary cerebral ischemia in the rat (Burnett et al., 2006), and a recent study found that vagal nerve stimulation during ischemia also reduces damage from transient cerebral ischemia (Ay et al., 2009). Since our previous study (Burnett et al., 2005) used only a single laser Doppler (LD) probe to monitor the intra-ischemic events, changes in cerebral blood flow (CBF) due to stimulation remains to be determined despite the promising results.

In the past decade optical imaging [laser speckle imaging (LSI) and imaging of intrinsic signals (OIS)] has became a powerful tool for collecting information on cortical perfusion and metabolism with excellent temporal and spatial resolution (Dunn et al., 2005). In the present study we have used multispectral (LSI and OIS) imaging to determine if contralateral forepaw stimulation in rat has any detectable biological effect on intra-ischemic CBF and/or flow/hemoglobin transients (Strong et al., 2007; Jones et al., 2008; Luckl et al., 2009) during focal brain ischemia.

MATERIALS AND METHODS

PHOTOCHEMICALLY INDUCED DISTAL MIDDLE CEREBRAL ARTERY OCCLUSION

All procedures performed were approved by the Institutional Animal Care and Use Committee of the University of Pennsylvania. Adult male Sprague–Dawley rats (290–320 g) were anesthetized with 4% isoflurane for induction in a mixture of 50% nitrous oxide and 50% oxygen and maintained on 1.2–1.3%

isoflurane (1.0–1.25 MAC) in 70% nitrous oxide and 30% oxygen during surgery and throughout the study. Body temperature was monitored by a rectal probe and maintained at 37.5 ± 0.2°C with a heating blanket regulated by a homeothermic blanket control unit (Harvard Apparatus Limited Holliston, MA, USA). A polyethylene catheter (PE-50) was placed into the tail artery for the measurement of arterial blood pressure and for blood gas sampling. Blood pressure was continuously monitored using a pressure transducer and recorded on a computer based recording system (PowerLab, ADInstruments, Colorado Springs, CO, USA). The right CCA was exposed by a ventral midline incision in the neck and the retraction of the sternocleidomastoid muscle. The exposed artery was surrounded by a snare. The rats were placed into a stereotaxic head holder, and a 6 × 6 mm area centered 3 mm posterior and 4 mm lateral to Bregma was thinned for laser speckle (**Figure 1**). Special attention was paid during surgical preparation to make the skull thickness uniform (Parthasarathy et al., 2008).

A 2-cm vertical incision was made midway between the right eye and the right ear. The temporalis muscle was separated and retracted to expose the zygomatic and squamosal bones. Under an operating microscope (Carl Zeiss, Inc.), a burr hole of 4 mm in diameter was made with a high-speed drill 1 mm rostral to the anterior junction of the zygomatic and squamosal bones, revealing the distal segment of the middle cerebral artery (MCA). The epidural temperature was monitored by probe and maintained at 37.5 ± 0.3°C with a custom-made air ventilator blowing warm air to the dura. The right side of the stereotaxic frame was tilted upward for the imaging and so that the laser could hit the vessel perpendicularly. A laser beam was focused on the artery through a spherical lens of 25 cm focal length. To induce occlusion, a stock solution of Erythosin B dye (MP Biomedicals, Solon, OH, USA), 17 mg/mL in 0.9% saline, was made for intravenous injection (via the tail vein) at a dose of 40 mg/kg. Immediately after injection of the dye, the MCA was irradiated (532 nm) for 5 min with a 4 mW beam from a diode laser (LaserGlow Technologies, model LRS-0532-KFM-00030-03). A thrombus was produced proximally to the Y-shaped juncture of the frontal and parietal branches of the MCA by focusing the laser at that site. An orange fluorescence was immediately observed in the irradiated distal MCA segment under the operating microscope. A white thrombus began to form approximately 4–5 min later within the fluorescent segment and gradually elongated distally. Following the irradiation, the right CCA was occluded permanently by tightening the snare. Since real time speckle imaging was started immediately after the injection of the erythrosin B, we could confirm successful occlusion also by real time flow measurement. Changes in oxygenation and blood flow were monitored through a thinned skull preparation with intrinsic optical imaging (Grinvald et al., 1986; Kohl et al., 2000) and speckle contrast imaging (Briers, 2001; Dunn et al., 2001; Durduran et al., 2004).

IMAGING

We obtained images of changes in CBF by measuring changes in speckle contrast (calculated using 7 × 7 pixel sliding window), C, of the raw speckle intensity images (Briers, 2001). Because the camera exposure time, T, was much greater than the speckle correlation time, τ_c, which is inversely proportional to the CBF (Bonner and Nossal, 1981), we used the simple relation $\tau_c = 2TC^2$ (Ramirez-San-Juan et al., 2008) to relate contrast to CBF. To improve the signal-to-noise ratio, 15 $1/\tau_c$ images were averaged together. Relative CBF images were then derived by normalizing the averaged $1/\tau_c$ images with baseline measurements obtained at the beginning of the data collection with a correction for biological zero ($1/\tau_c$ values when cerebral perfusion was zero) (Ayata et al., 2004; Strong et al., 2006; Zhou et al., 2008). In this study, biological zero images could not be obtained in each animal because the animals were not sacrificed until days after the imaging. Consequently, a group of animals ($n = 6$) was used to determine the biological zero value, which was found to be 9.1 ± 1.2% of baseline.

To monitor oxygenation with intrinsic optical imaging, we acquired spectral intensity images at three wavelengths (540, 580, and 610 nm) and used a modified Beer–Lambert relationship (Arridge et al., 1992) to relate the reflectance attenuation at each wavelength to changes in hemoglobin concentration. In this analysis, we assumed that contributions to the attenuation from chromophores other than oxyhemoglobin (HbO) and deoxyhemoglobin (Hb) and changes in scattering over the wavelength range used are negligible. Furthermore, we generated the differential pathlength factors in the modified Beer–Lambert relation using Monte Carlo simulations that included the geometry of the imaging system (Kohl et al., 2000).

Our imaging instrument is very similar to the one previously described by (Dunn et al., 2003). For speckle imaging, a collimated laser diode (DL7140-201S, 785 nm, 80 mW; Thorlabs, Newton, NJ, USA) driven by a commercial laser diode controller (LDC 500; Thorlabs, Newton, NJ, USA) provided uniform illumination on the skull surface. To acquire spectral images at multiple-wavelengths, a xenon arc lamp (XBO 150 W/1 OFR; OSRAM) was directed through an eight-position filter wheel (FW-1000, Applied Scientific Instrumentation, Inc) and then coupled to a 12-mm fiber bundle illuminating the cortex. The filter wheel was programmed such that external trigger pulses consecutively switched the filter wheel between four positions. Three positions contained 10-nm bandpass filters centered at wavelengths of 540, 580, and 610 nm, with the other position blocked. The laser diode was off while the filter wheel was in the first three positions, but switched on when the filter wheel reached the blocked position, enabling interleaved spectral and speckle imaging with 140 μm spatial resolution every 2 s.

Imaging software (StreamPix; NorPix, Montreal, Quebec, Canada) was used to record images over the right MCA territory acquired by a 12-bit, TEC cooled CCD camera (Uniq; Uniq Vision Inc.) with a field of view of 5 × 5 mm. A 60-mm lens (Schneider-Kreuznach, Apo-Componon 2.8/40, Germany) was used to focus the image, and the aperture was adjusted so that the speckle size matched the pixel dimensions (9.9 × 9.9 μm). Every 2 s, three spectral and 15 speckle images were taken. A program written in the SciWorks software environment (DataWave Technologies, Boulder, CO, USA) that interfaces to an A/D board controlled the timing for the external triggering of the camera and filter wheel, as well as the timing for switching on/off the laser diode.

CALCULATION OF OXYGEN METABOLISM CHANGES

Relative changes in the cerebral metabolic rate of oxygen ($rCMRO_2$) were calculated from the images of CBF, total hemoglobin, and deoxyhemoglobin using the relationship (Mayhew et al., 2000; Jones et al., 2001):

$$rCMRO_2 = \left(1+\frac{\Delta CBF}{CBF_0}\right)\left(1+\gamma_r\frac{\Delta Hb}{Hb_0}\right)\left(1+\gamma_t\frac{\Delta HbT}{HbT_0}\right)^{-1}-1,$$

where the subscript "o" indicates baseline values and the symbol "Δ" indicates changes from baseline values. The parameters γ_r and γ_t are vascular weighting constants proportional to the amount of deoxyhemoglobin and total hemoglobin in venules, respectively, and are assumed to be one in our calculation. Also, while speckle measures relative changes in CBF directly, OIS cannot determine absolute concentrations, so we assumed baseline values of 60 and 40 μM for HbT_0 and Hb_0, respectively (Dunn et al., 2005). The equation for $rCMRO_2$ was derived based on direct measurements of changes in CBF, deoxyhemoglobin and total hemoglobin in the venous compartment. It is assumed, however, that the optical signal from the brain is proportional to that in the venous compartment and further that the relative volume fractions of the arteriole, capillary, and venules compartments does not change. We have shown that this equation is relatively insensitive to changes in these volume fractions (Culver et al., 2003) although in the core of the ischemia the changes may be more appreciably. The flow transients (where $rCMRO_2$ has been calculated) are not in the most ischemic regions and consequently errors based on this assumption are small.

TEMPORAL PROTOCOL AND IMAGE ANALYSIS

Prior to the initiation of imaging, two subdermal electrodes were inserted into the left (contralateral to injury) forepaw between digits 1 and 2 and between 3 and 4. After 5 min of collecting baseline flow and oxygenation data, a 15-min data collection of real time speckle was initiated synchronously with the production of photothrombosis in order to confirm a successful occlusion (**Figure 2**). The occlusion usually occurred in the 4–5th min of the real time speckle sequence. In the remaining 10-min CBF was monitored to exclude the chance of spontaneous reperfusion. After confirming the successful, reperfusion-free occlusion, surface blood flow, and oxygenation were monitored in 15 min long intra-ischemic sequences over a period of 2 h. Laser speckle (15 Hz) and three-wavelength OIS (540, 580, 610 nm) data were obtained every 2 s. Seven animals underwent 2-h forepaw stimulation (2-mA pulses, 5 Hz for 4 s with 3-s rest) starting with the first intra-ischemic (LS + OIS) sequence synchronously and continuing for 120 min, while seven animals did not receive forepaw stimulation. Data from the literature indicate that a 2 mA forepaw electrical stimulus is innocuous (Luo et al., 2009).

The high spatial resolution images were divided into nine equal sectors, and one circular region of interest (ROI, 0.3 mm in diameter; **Figure 1**) was placed in each sector, where care was taken to ensure the ROIs were not over any large blood vessels. Changes in blood flow, hemoglobin, and metabolism in each ROI over time were analyzed.

The average residual cerebral blood flow (rCBF) during the first 120 min of ischemia was calculated as a percentage of the baseline (5 min) prior to the occlusion over each ROI. Both hemoglobin and peri-infarct flow transients (PIFT) were identified by their propagating feature (transients seen in at least two ROIs with appropriate time delay). The occurrence of flow transients over each ROI was calculated as the percentage of the total number of flow transients in each experimental group (Strong et al., 2007; Jones et al., 2008; Luckl et al., 2009). The duration of the flow transients was determined by computing a mean of the laser speckle signal 1 min both prior to and following a peri-infarct flow transient, and then determining the start and the end of the PIFT from the time at which the mean laser speckle signal intercrossed with the ascending or the descending leg of the PIFT (Luckl et al., 2009). The amplitude was obtained as the percent change in CBF. We measured the hypoperfusion and hyperemia components of the amplitudes separately. The duration and the amplitudes of the Hb (Hb, HbO) transients and $CMRO_2$ changes were determined similarly.

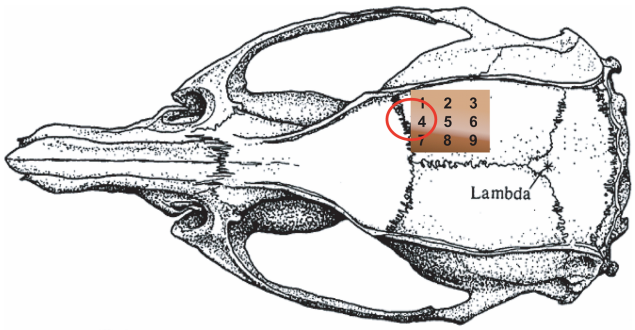

FIGURE 1 | Schematic figure of the thinned skull with the positions of the nine regions of interests (ROI). The shadowing (white line) shows the border zone of the lesion in both groups of animals (no significant difference) after mapping the infarct area with the map of ROIs. The red ellipse indicates the cortical representation of the forepaw as determined by blood oxygen-level dependent imaging (Ghosh et al., 2009) and by OIS in our laboratory.

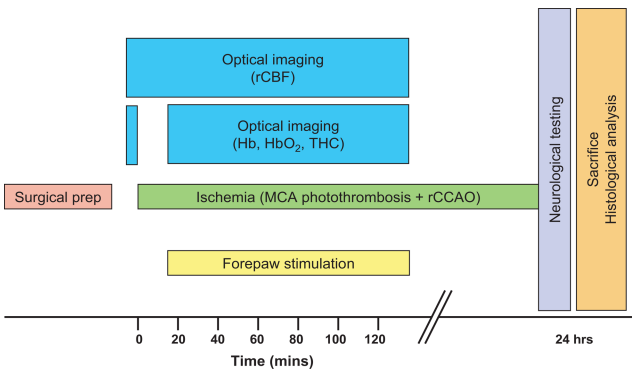

FIGURE 2 | Schematic of study design. Ischemia was produced by direct occlusion of the right middle cerebral artery (MCA) by photothrombosis along with right common carotid artery occlusion (rCCAO), and optical imaging was done during the acute phase of ischemia.

NEUROLOGICAL EVALUATION AND INFARCT VOLUME MEASUREMENT

A neurological evaluation was performed at 24 h post-injury according to the protocol of (De Ryck et al., 1989). Visual placing in forward and sideways directions, tactile placing of the dorsal

and lateral paw surfaces, and proprioceptive placing were tested and scored on a 10-point scale ranging from 10 (no deficit) to 0 (maximum deficit).

Rats were sacrificed 24 h after MCAO. The brain was removed from the skull and was sectioned in the coronal plane at 1.5-mm intervals using a rodent brain matrix. The brain slices were stained with 2% triphenyltetrazolium chloride (TTC), photographed and the infarct volume was determined as described previously (Luckl et al., 2007). We also mapped the infarcted area to the imaging data. The distance between the midline and the border of the infarct zone on the TTC slices was measured and mapped onto the flow and hemoglobin images. According to our sectioning method slices from No. 2 to No. 5 correspond to the thinned area on the skull.

STATISTICAL ANALYSIS

The physiological parameters (baseline and intra-ischemic), the outcomes (infarct size, edema), and the number of flow transients were tested using two-way repeated-measures analysis of variance (ANOVA). When differences were found, a Holm–Sidak test was conducted to probe the origin of differences (control vs stimulated, baseline vs ischemia) and to correct for multiple tests. Neurological scores were examined with a Mann–Whitney rank sum test. A two-way ANOVA with repeated-measures analysis was used to statistically exclude presence of regional heterogeneity in the baseline flow and to compare the mean amplitude of the hemoglobin (oxy, deoxy) transients and the related $CMRO_2$ changes. Region and group (stimulated, non-stimulated) were the independent variables and hemoglobin and $CMRO_2$ transients were dependent variables.

RESULTS

PHYSIOLOGICAL VARIABLES

The physiological variables were in a normal range in each animal (**Table 1**). There were no significant differences in any parameter between the control and stimulated groups. However, occlusion did produce a significant increase in MABP ($p < 0.01$) independent of group (control, stimulated), but in no other physiological parameter did occlusion significantly produces changes.

Table 1 | Physiological variables.

	Control	Stimulated
BASELINE		
Weight (g)	309 ± 19	298 ± 15
MABP (mm Hg)	91 ± 8	97 ± 6
pH	7.46 ± 0.03	7.43 ± 0.04
PO_2 (mm Hg)	126 ± 14	130 ± 24
PCO_2 (mm Hg)	35.9 ± 4.7	39.6 ± 4.9
Core temp (°C)	37.5 ± 0.2	37.5 ± 0.2
Dura temp (°C)	37.5 ± 0.3	37.4 ± 0.3
ISCHEMIA (20 MIN POST-MCAO)		
MABP (mm Hg)	114 ± 15	118 ± 9
pH	7.46 ± 0.04	7.45 ± 0.03
PO_2 (mm Hg)	122 ± 21	122 ± 14
PCO_2 (mm Hg)	35.1 ± 4.9	36.0 ± 5.0
Core temp (°C)	37.6 ± 0.2	37.4 ± 0.2
Dura temp (°C)	37.5 ± 0.2	37.5 ± 0.2
ISCHEMIA (80 MIN POST-MCAO)		
MABP (mm Hg)	113 ± 13	118 ± 8
pH	7.45 ± 0.03	7.44 ± 0.03
PO_2 (mm Hg)	119 ± 18	121 ± 11
PCO_2 (mm Hg)	36.61 ± 3.1	34.2 ± 4.3
Core temp (°C)	37.6 ± 0.2	37.5 ± 0.2
Dura temp (°C)	37.5 ± 0.2	37.5 ± 0.1

Mean ± SD.

HISTOLOGICAL AND NEUROLOGICAL OUTCOME

Both the neurological (sham: 3.6 ± 1.7, stimulated: 4.3 ± 1.4) and the histological (sham: 124 ± 39 mm^3, stimulated: 147 ± 47 mm^3) outcome did not show significant difference between stimulated and control groups. By mapping the infarct zone with the ROI map we found that ROI 7, 8, 9 represents the peri-ischemic area in both groups.

CEREBRAL BLOOD FLOW AND PERI-INFARCT FLOW TRANSIENTS

Two-way ANOVA with repeated measures (animal and ROI) showed that there was a difference in residual blood flow after occlusion between the peri-ischemic area (ROI 7–9) and the ischemic cortex (ROI 1–6) ($p < 0.002$), but no difference between stimulated and non-stimulated animals ($p = 0.658$). The results of laser speckle imaging are presented in **Table 2**. The averaged residual flow after the occlusion was between 47% and 58% of baseline in both groups over the peri-ischemic area. Similarly, there were no differences in residual flow (26–35%) between groups over the ischemic cortex.

The averaged number of flow transients were significantly ($p < 0.05$) higher in the forepaw-stimulated animals (7.0 ± 2.3) compared to the non-stimulated group (3.5 ± 2.3). The flow transients propagate mostly over the peri-ischemic (ROI 7–9) and the penumbral (ROI 4–6) region while the occurrence of flow transients is very low over ROI 1–3 which probably represents the core.

We could distinguish five different morphologies of flow transients as described previously (Luckl et al., 2009). Briefly: (I) monophasic, hyperemic; (II, III) biphasic (hyperemia or hypoperfusion dominant); and (IV, V) monophasic, hypoperfusive (transient or prolonged). The propagation of the flow transients was multi-directional, sometimes giving the impression of being "disordered". In one case, the propagation was bi-directional (splitting) and in another case, a hyperemic, low frequency flow oscillation could be seen over a well-circumscribed part of the ischemic cortex. In early studies with this model we saw the whole cycling propagation pattern described by Graf et al. (2007) in only a few animals probably because we used a representative, but relatively small, "window" size compared to the complete ischemic territory.

HEMOGLOBIN/$CMRO_2$ TRANSIENTS

Tables 3 and 4 summarize the results of OIS imaging. Since the occurrence of transients is very low over the "core" region (ROI 1–3) (**Table 2**) we only examined the data coming from ROI 4–9 in the statistical analysis. Forepaw stimulation significantly ($p < 0.05$) reduces the transient-related $CMRO_2$ changes over ROI 4–9 (penumbra and peri-ischemic area). In concert with this result, we found

Table 2 | Results of laser speckle imaging in the control- (non-stimulated) and forepaw-stimulated groups.

	Control animals			Stimulated animals		
ROI	**rCBF* (%)**	**Occurrence of PIFT** (%)**	**Average duration of PIFT (s)**	**rCBF**	**Occurrence of PIFT (%)**	**Average duration of PIFT (s)**
1	26 ± 7	12	220 ± 40	31 ± 12	8	210 ± 40
2	28 ± 13	8	211 ± 23	29 ± 12	4	201 ± 38
3	27 ± 9	4	222 ± 45	29 ± 15	4	187 ± 20
4	33 ± 16	52	212 ± 43	35 ± 12	49	220 ± 44
5	28 ± 9	32	230 ± 45	30 ± 16	39	242 ± 54
6	33 ± 13	32	242 ± 51	35 ± 12	45	246 ± 50
7	53 ± 18	100	256 ± 59	58 ± 12	100	260 ± 72
8	47 ± 9	100	217 ± 55	48 ± 13	100	250 ± 42
9	54 ± 8	96	227 ± 52	57 ± 18	94	242 ± 56

**Average relative cerebral blood flow (rCBF) over the first 120 min of ischemia as a percent of pre-ischemic flow*
***Frequency of peri-infarct flow transients (PIFT) in region of interest (ROI) as a percent of total number of PIFTs in the group.*

Table 3 | Changes in oxygen concentrations and cerebral oxygen metabolism in animals during forepaw stimulation (mean ± SD).

	Parameters	**ROI_4**	**ROI_5**	**ROI_6**	**ROI_7**	**ROI_8**	**ROI_9**
$CMRO_2$	Change %	30.9 ± 9.1	26.7 ± 8.1	22.4 ± 3.7	34.3 ± 9.4	35.4 ± 3.9	36.7 ± 10.6
HbO	Amplitude (μM)	15 ± 12.4	12.2 ± 9.4	7.6 ± 1.6	20.4 ± 12.9	23.2 ± 10.3	19.4 ± 6.7
	Duration (s)	262 ± 100	248 ± 54	246 ± 48	250 ± 74	260 ± 30	232 ± 54
Hb	Amplitude (μM)	5.9 ± 1.1	6.5 ± 1.5	4.4 ± 1.1	6.9 ± 1.1	6.4 ± 1.1	7.7 ± 2.3
	Duration (s)	252 ± 7.2	230 ± 42	256 ± 46	202 ± 44	176 ± 18	174 ± 30

Table 4 | Change in oxygen concentrations and cerebral oxygen metabolism in control animals (mean ± SD).

	Parameters	**ROI_4**	**ROI_5**	**ROI_6**	**ROI_7**	**ROI_8**	**ROI_9**
$CMRO_2$	Change %	47.6 ± 8.8	35.8 ± 5.0	32.6 ± 5.0	46.4 ± 12.3	48.2 ± 9.6	47 ± 13.7
HbO	Amplitude (μM)	22 ± 19.1	17.1 ± 2.6	27.4 ± 2.7	33 ± 15.7	29.9 ± 13.5	20.3 ± 9.3
	Duration (s)	234 ± 80	276 ± 32	292 ± 54	284 ± 76	282 ± 68	270 ± 56
Hb	Amplitude (μM)	9.9 ± 7.4	7.4 ± 3.5	7.5 ± 3.3	9.9 ± 4.3	7.8 ± 2.7	8.1 ± 2.3
	Duration (s)	254 ± 44	252 ± 66	278 ± 89	200 ± 32	170 ± 40	196 ± 78

also that the mean amplitude (peak to peak) of oxy and deoxy Hb transients were smaller in the stimulated animals, although these differences were not significant (**Figures 3 and 4**). We also did not find significant differences between groups with respect to the average duration of hemoglobin (oxy, deoxy) transients.

DISCUSSION

Our study provides a multispectral, optical imaging analysis of intra-ischemic CBF and metabolism during contralateral forepaw stimulation. The results show that forepaw stimulation can significantly modify the number of PIFT and the transients-related metabolic load in the ischemic hemisphere (contralateral to stimulated forepaw).

Although, our previous study (Burnett et al., 2006) clearly showed that forepaw stimulation has neuroprotective effect in transient focal ischemia, the present study in permanent ischemia did not demonstrate differences in outcome measurements between groups. It should be stressed that this study was designed only to look for any possible biological effect of contralateral forepaw stimulation. We produced a permanent ischemia by photothrombosis, but applied forepaw stimulation only for 2 h. The photothrombosis model of distal MCA occlusion was chosen since it allowed for the dura to remain intact during the surgery and therefore was less invasive than more direct MCA occlusion techniques for the production of permanent focal cerebral ischemia (Chen et al., 1986).

The original hypothesis on the possible beneficial effect of contralateral forepaw stimulation in ischemia was that functional stimulation might increase the intra-ischemic blood flow through collaterals. When we did not see any significant blood flow change in our original study (Burnett et al., 2006) in which a single laser Doppler probes was positioned over the ischemic region, we attributed this to the fact that only a single small region in the MCA was sampled. Similarly, we could not see increase in flow by laser speckle

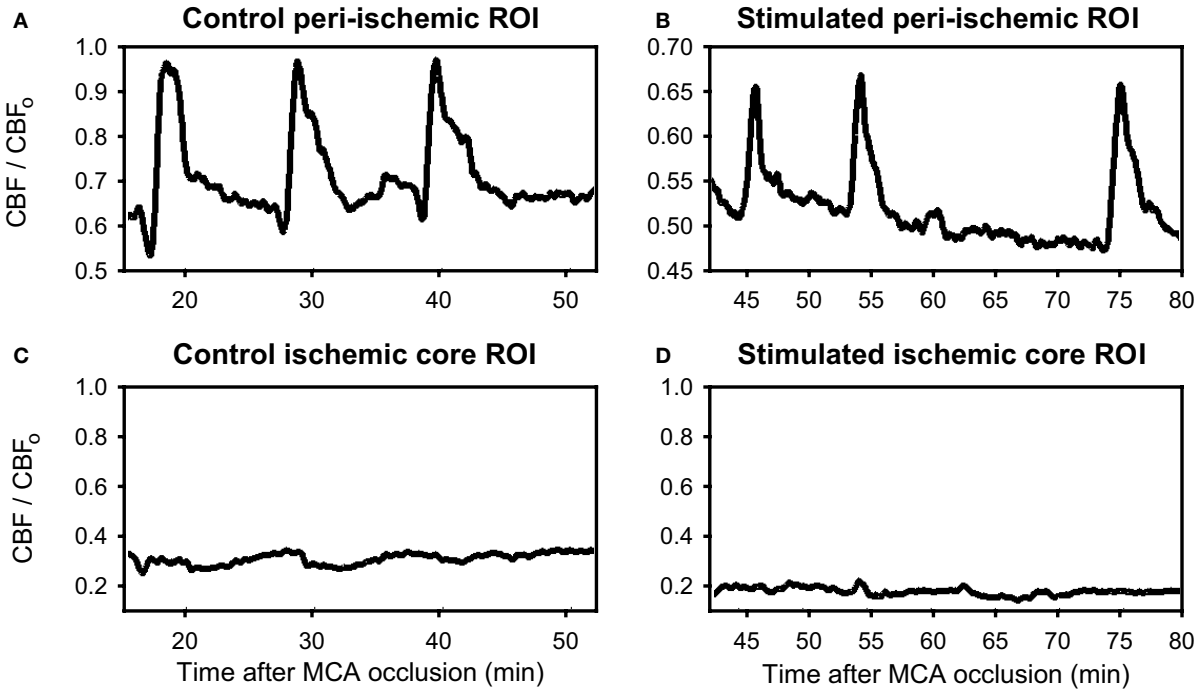

FIGURE 3 | Demonstration of flow transients in relative cerebral blood flow (CBF/CBF$_o$) in peri-ischemia regions. (A, B) and in the ischemic core **(C, D)** from a typical rat not receiving forepaw stimulation during ischemia **(A, C)** and from a rat receiving forepaw stimulation during ischemia **(B, D).** The "o" subscript refers to the parameter prior to MCA occlusion. Note the significant flow transients in the peri-ischemic territory (ROIs 7–9), whereas the occurrence of the transients over the ischemic core (ROIs 1-3) was very low.

in the forepaw-stimulated animals in the present study. There was no significant difference in residual flow between groups even over the peri-ischemic (ROI 7–9, watershed zone between MCA and anterior cerebral artery) region.

The averaged number of flow transients, however, was significantly higher in the forepaw-stimulated animals. In addition, we also found that the mean amplitude of oxy- and deoxy Hb transients was smaller although non-significantly in the stimulated animals, and forepaw stimulation significantly reduced the transient-related $CMRO_2$ changes over ROI 4–9 (penumbra and peri-ischemic area). It is important to note that we detected these changes over the whole (6×6 mm) monitored region which is larger than the cortical representation area of the forepaw (**Figure 1**). This significant "mismatch" indicates at first sight that the underlying mechanism is probably not related to a possible input of stimulation into the ischemic cortex. However, data from the literature suggest that the flow transients show a cyclic propagation pattern around the core. Although our "window" was relatively small for detecting the full circling pattern, our data suggest that a significant proportion of flow transients propagate through the forepaw area. Our results also indicate that at least a part of the forepaw area is peri-ischemic with rCBF over 50% of baseline. Such level of ischemia still allows synaptic activity and some cortical input (Hossmann, 1994; Burnett et al., 2005). We speculate that the forepaw area in the cortex may include a small territory at the ACM–ACA watershed zone where spreading depolarizations and the corresponding flow/hemoglobin transients can be modified through electrical stimulation.

In various animal models of cerebrovascular disease, spreading depolarization (SD) has been found to contribute to ischemic injury through its high metabolic and excitotoxic impact (Nedergaard and Astrup, 1986). SDs increase cerebral metabolic rate by 71% (Piilgaard and Lauritzen, 2009) in non-ischemic rat cortex. The metabolic load due to the transients in our control animals over the peri-ischemic cortex with CBF around 50% of control was 46–48% while the $CMRO_2$ change was 30–35% over the penumbra. Forepaw stimulation decreases this metabolic load significantly by 30–45% over both penumbral and peri-ischemic tissue.

The expansion of the core coincides with the occurrence of repetitive spreading depolarizations (Hossmann, 1996; Shin et al., 2006). In a distal MCAO model of mice each subsequent spreading depolarization expanded the core by an additional 19% (Shin et al., 2006). Our experience with filament occlusion in rat shows that the number of flow transients clearly correlate with the histological outcome but not in a definite stepwise fashion (Luckl et al., 2009). Similarly, NADH fluorescence studies in focal ischemia showed that recurrent depolarization increases the severity of neuronal injury but only a proportion of spreading depolarizations enlarge the core (Higuchi et al., 2002; Sasaki et al., 2009). In the present study we found that the number of flow transients were significantly higher in the stimulated group. Taking the outcome measurements into consideration, it is likely that a certain percent of transients with the decreased metabolic load is non-injurious. Whether forepaw stimulation increases the "real" number of transients or increases only the speed of these transients around the core remains unanswered in this study.

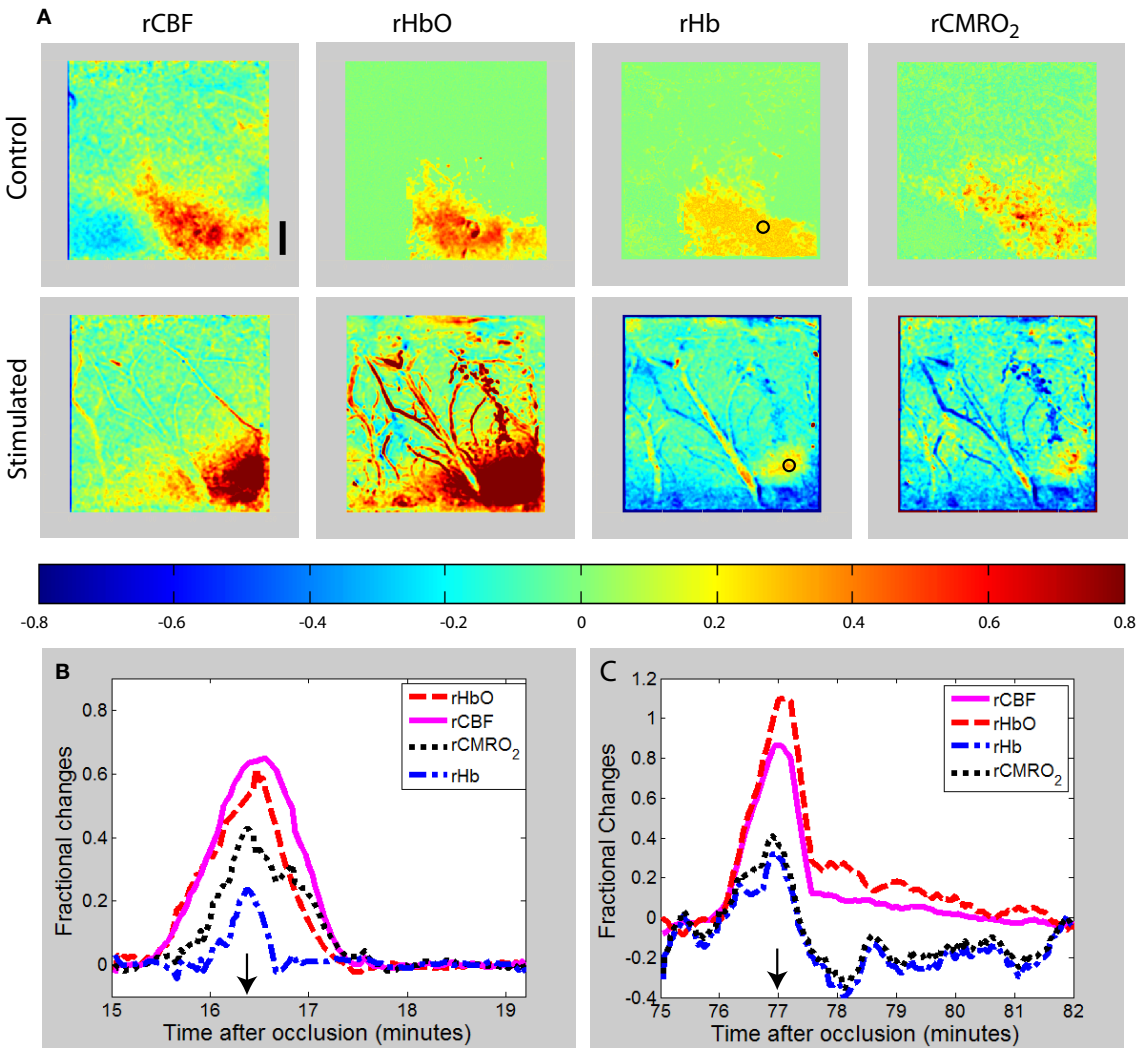

FIGURE 4 | (A) Maps of changes in relative blood flow (rCBF), relative oxyhemoglobin (rHbO), relative deoxyhemoglobin (rHb), and relative oxygen consumption ($rCMRO_2$) during a transient in the peri-ischemia cortex of a exemplar control (non-stimulated) and forepaw-stimulated animal. In both animals, the transient is moving toward the right of the image (caudally). The color bar indicates fractional decreases or increases of each parameter with respect to its level just prior to the start of the transient. The time course of the parameters for the region of interest shown by the circular ROI in the rHb images is shown for the control **(B)** and stimulated **(C)** animal, with the images shown in **(A)** obtained at the time indicated by the arrows. Scale bar is 1 mm.

The site of the MCA occlusion may influence the outcome of the experiment. With this model (distal photothrombotic occlusion of the MCA) we found that the propagation of the flow/Hgb transients was confined mostly to ROI 7–9. In a filament occlusion study (proximal occlusion of the MCA) with a "window" in a similar position, we found that the propagation pattern of the PIFTs is more conservative (fronto-caudal) with the transients traveling through the entire observational area and the occurrence of the flow transients being close to 100% over each ROI (Luckl et al., 2009). The explanation might be that the distal occlusion of the MCA induces an infarct only in the parietal lobe while the proximal MCAO affects a larger volume (parietal and temporal lobe) making the diameter and the extent of the presumed cycling larger. Taking into consideration that the location and the extent of the forepaw area may vary in animals, the chance that a flow transient propagates through the forepaw area and that it can be modulated by forepaw stimulation is presumably higher in proximal MCAO than in the distal MCAO model. Differences in hemodynamics in different stroke models may also determine the effect of stimulation. For example distal occlusion of the MCA leaves the proximal branches patent while these are closed during proximal MCA occlusion (filament occlusion). The inability to see any appreciable increases in the present study using imaging, which monitors a large region does suggest that forepaw stimulation during photothrombotic occlusion of the distal MCA in the rat does not increase blood flow in the ischemic or peri-ischemic territory. This is not to say that blood flow would not be altered in other focal ischemia models.

Strictly speaking, the theory of laser speckle imaging assumes that the speckle intensities over time are Gaussian with mean zero (Lemieux and Durian, 1999). This assumption breaks down in the

presence of static scatterers, such as the thinned skull of the rat, because the speckle pattern due to static scattering is constant over time. Several methods have been proposed to account for the presence of static scattering when doing speckle imaging (Li et al., 2006; Zakharov et al., 2006; Parthasarathy et al., 2008; Zakharov et al., 2009). We employed Zakharov et al.'s algorithm, which determines the static contribution in the speckle pattern by cross-correlating sequential speckle images (Zakharov et al., 2009). Based on our findings, neglecting the effect of the skull and other static scattering elements introduces a systematic underestimation in flow changes of less than 5%. However, this would not affect the conclusions when comparing the transients between stimulation and control groups.

The equation used to calculate changes in $CMRO_2$ is based on many assumptions (Culver et al., 2003; Jones et al., 2008) which may not be valid in ischemia, and particularly in the ischemic core. For this reason, we have limited our calculations of $rCMRO_2$ to the peri-ischemic and penumbral portions of the cortex. The derivation of this equation assumes that the volume fraction of the vascular compartments (arteriole, capillary, venule) from which the optical signal originates does not change. In a previous publication we argue that ischemia can lead to a 9–21% underestimation in the calculated $rCMRO_2$ (Culver et al., 2003). However, since the changes in the microvascular hemodynamics appear to be similar in the stimulated and non-stimulated animals, these errors will be comparable and our conclusions will not be significantly affected.

With multispectral optical imaging we have taken the first step in deciphering the possible influence of forepaw stimulation on ischemic tissue. Based on the results we speculate that forepaw stimulation exerts its effect probably through the cortical representation of the forepaw by modulating the nature of the propagating flow/metabolic transients. The next step would be to investigate the impact of a different stimulation paradigm (increasing frequency or amplitude, etc.). Since we did not record DC potentials it would be also important to check the effect of stimulation directly on spreading depolarizations especially over the forepaw area.

ACKNOWLEDGMENT

This study was supported by National Institutes of Health grant NS057400.

REFERENCES

Arridge, S. R., Cope, M., and Delpy, D. T. (1992). The theoretical basis for the determination of optical pathlengths in tissue: temporal and frequency analysis. *Phys. Med. Biol.* 37, 1531–1560.

Ay, I., Lu, J., Ay, H., and Gregory, S. A. (2009). Vagus nerve stimulation reduces infarct size in rat focal cerebral ischemia. *Neurosci. Lett.* 459, 147–151.

Ayata, C., Dunn, A. K., Gursoy-OZdemir, Y., Huang, Z., Boas, D. A., and Moskowitz, M. A. (2004). Laser speckle flowmetry for the study of cerebrovascular physiology in normal and ischemic mouse cortex. *J. Cereb. Blood Flow Metab.* 24, 744–755.

Bonner, R., and Nossal, R. (1981). Model for laser Doppler measurements of blood flow in tissue. *Appl. Optics* 20, 2097–2107.

Briers, J. D. (2001). Laser Doppler, speckle and related techniques for blood perfusion mapping and imaging. *Physiol. Meas.* 22, R35–R66.

Brown, J. A., Lutsep, H. L., Weinand, M., and Cramer, S. C. (2006). Motor cortex stimulation for the enhancement of recovery from stroke: a prospective, multicenter safety study. *Neurosurgery* 58, 464–473.

Burnett, M. G., Detre, J. A., and Greenberg, J. H. (2005). Activation-flow coupling during graded cerebral ischemia. *Brain Res.* 1047, 112–118.

Burnett, M. G., Shimazu, T., Szabados, T., Muramatsu, H., Detre, J. A., and Greenberg, J. H. (2006). Electrical forepaw stimulation during reversible forebrain ischemia decreases infarct volume. *Stroke* 37, 1327–1331.

Chae, J., Sheffler, L., and Knutson, J. (2008). Neuromuscular electrical stimulation for motor restoration in hemiplegia. *Top. Stroke Rehabil.* 15, 412–426.

Chen, S. T., Hsu, C. Y., Hogan, E. L., Maricq, H., and Balentine, J. D. (1986). A model of focal ischemic stroke in the rat: reproducible extensive cortical infarction. *Stroke* 17, 738–743.

Culver, J. P., Durduran, T., Furuya, D., Cheung, C., Greenberg, J. H., and Yodh, A. G. (2003). Diffuse optical tomography of cerebral blood flow, oxygenation, and metabolism in rat during focal ischemia. *J. Cereb. Blood Flow Metab.* 23, 911–924.

De Ryck, M., Van, R. J., Borgers, M., Wauquier, A., and Janssen, P. A. (1989). Photochemical stroke model: flunarizine prevents sensorimotor deficits after neocortical infarcts in rats. *Stroke* 20, 1383–1390.

Dunn, A. K., Bolay, H., Moskowitz, M. A., and Boas, D. A. (2001). Dynamic imaging of cerebral blood flow using laser speckle. *J. Cereb. Blood Flow Metab.* 21, 195–201.

Dunn, A. K., Devor, A., Bolay, H., Andermann, M. L., Moskowitz, M. A., Dale, A. M., and Boas, D. A. (2003). Simultaneous imaging of total cerebral hemoglobin concentration, oxygenation, and blood flow during functional activation. *Opt. Lett.* 28, 28–30.

Dunn, A. K., Devor, A., Dale, A. M., and Boas, D. A. (2005). Spatial extent of oxygen metabolism and hemodynamic changes during functional activation of the rat somatosensory cortex. *Neuroimage* 27, 279–290.

Durduran, T., Burnett, M. G., Yu, G., Zhou, C., Furuya, D., Yodh, A. G., Detre, J. A., and Greenberg, J. H. (2004). Spatiotemporal quantification of cerebral blood flow during functional activation in rat somatosensory cortex using laser-speckle flowmetry. *J. Cereb. Blood Flow Metab.* 24, 518–525.

Ghosh, A., Sydekum, E., Haiss, F., Peduzzi, S., Zorner, B., Schneider, R., Baltes, C., Rudin, M., Weber, B., and Schwab, M. E. (2009). Functional and anatomical reorganization of the sensory-motor cortex after incomplete spinal cord injury in adult rats. *J. Neurosci.* 29, 12210–12219.

Graf, R., Nakamura, H., Vollmar, S., Dohmen, C., Sakawitz, B., Bosche, B., Dunn, A., and Strong, A. J. (2007). Cycling propagation of spontaneous spreading depolarizations around ischemic foci: evidence from experimental and clinical assessments. Program No. 765. 9 2007 Neuroscience Meeting Planner. San Diego, CA: Society for Neuroscience. Online.

Grinvald, A., Segal, M., Kuhnt, U., Hildesheim, R., Manker, A., Anglister, L., and Freeman, J. A. (1986). Real-time optical mapping of neuronal activity in vertebrate CNS in vitro and in vivo. *Soc. Gen. Physiol Ser.* 40, 165–197.

Higuchi, T., Takeda, Y., Hashimoto, M., Nagano, O., and Hirakawa, M. (2002). Dynamic changes in cortical NADH fluorescence and direct current potential in rat focal ischemia: relationship between propagation of recurrent depolarization and growth of the ischemic core. *J. Cereb. Blood Flow Metab.* 22, 71–79.

Hossmann, K. A. (1994). Viability thresholds and the penumbra of focal ischemia. *Ann. Neurol.* 36, 557–565.

Hossmann, K. A. (1996). Periinfarct depolarizations. *Cerebrovasc. Brain Metab. Rev.* 8, 195–208.

Jones, M., Berwick, J., Johnston, D., and Mayhew, J. (2001). Concurrent optical imaging spectroscopy and laser-Doppler flowmetry: the relationship between blood flow, oxygenation, and volume in rodent barrel cortex. *Neuroimage* 13, 1002–1015.

Jones, P. B., Shin, H. K., Boas, D. A., Hyman, B. T., Moskowitz, M. A., Ayata, C., and Dunn, A. K. (2008). Simultaneous multispectral reflectance imaging and laser speckle flowmetry of cerebral blood flow and oxygen metabolism in focal cerebral ischemia. *J. Biomed. Optics* 13, 044007.

Kohl, M., Lindauer, U., Royl, G., Kuhl, M., Gold, L., Villringer, A., and Dirnagl, U. (2000). Physical model for the spectroscopic analysis of cortical intrinsic optical signals. *Phys. Med. Biol.* 45, 3749–3764.

Lemieux, P., and Durian, D. (1999). Investigating non-Gaussian scattering processes by using nth-order intensity correlation functions. *J. Opt. Soc. Am.* 16, 1651–1664.

Li, P., Ni, S., Zhang, L., Zeng, S., and Luo, Q. (2006). Imaging cerebral blood flow through the intact rat skull with temporal laser speckle imaging. *Opt. Lett.* 31, 1824–1826.

Luckl, J., Keating, J., and Greenberg, J. H. (2007). Alpha-chloralose is a suitable anesthetic for chronic focal cerebral ischemia studies in the rat: a comparative study. *Brain Res.* 1191, 157–167.

Luckl, J., Zhou, C., Durduran, T., Yodh, A. G., and Greenberg, J. H. (2009). Characterization of periinfarct flow transients with laser speckle and

Doppler after middle cerebral artery occlusion in the rat. *J. Neurosci. Res.* 87, 1219–1229.

Luo, Z., Yu, M., Smith, S. D., Kritzer, M., Du, C., Ma, Y., Volkow, N. D., Glass, P. S., and Benveniste, H. (2009). The effect of intravenous lidocaine on brain activation during non-noxious and acute noxious stimulation of the forepaw: a functional magnetic resonance imaging study in the rat. *Anesth. Analg.* 108, 334–344.

Mayhew, J., Johnston, D., Berwick, J., Jones, M., Coffey, P., and Zheng, Y. (2000). Spectroscopic analysis of neural activity in brain: increased oxygen consumption following activation of barrel cortex. *Neuroimage* 12, 664–675.

Nedergaard, M., and Astrup, J. (1986). Infarct rim: effect of hyperglycemia on direct current potential and [14C]2-deoxyglucose phosphorylation. *J. Cereb. Blood Flow Metab.* 6, 607–615.

Parthasarathy, A. B., Tom, W. J., Gopal, A., Zhang, X., and Dunn, A. K. (2008). Robust flow measurement with multi-exposure speckle imaging. *Opt. Express* 16, 1975–1989.

Piilgaard, H., and Lauritzen, M. (2009). Persistent increase in oxygen consumption and impaired neurovascular coupling after spreading depression in rat neocortex. *J. Cereb. Blood Flow Metab.* 29, 1517–1527.

Ramirez-San-Juan, J. C., Ramos-Garcia, R., Guizar-Iturbide, I., Martinez-Niconoff, G., and Choi, B. (2008). Impact of velocity distribution assumption on simplified laser speckle imaging equation. *Opt. Express* 16, 3197–3203.

Sasaki, T., Takeda, Y., Taninishi, H., Arai, M., Shiraishi, K., and Morita, K. (2009). Dynamic changes in cortical NADH fluorescence in rat focal ischemia: evaluation of the effects of hypothermia on propagation of peri-infarct depolarization by temporal and spatial analysis. *Neurosci. Lett.* 449, 61–65.

Shin, H. K., Dunn, A. K., Jones, P. B., Boas, D. A., Moskowitz, M. A., and Ayata, C. (2006). Vasoconstrictive neurovascular coupling during focal ischemic depolarizations. *J. Cereb. Blood Flow Metab.* 26, 1018–1030.

Strong, A. J., Anderson, P. J., Watts, H. R., Virley, D. J., Lloyd, A., Irving, E. A., Nagafuji, T., Ninomiya, M., Nakamura, H., Dunn, A. K., and Graf, R. (2007). Peri-infarct depolarizations lead to loss of perfusion in ischaemic gyrencephalic cerebral cortex. *Brain* 130, 995–1008.

Strong, A. J., Bezzina, E. L., Anderson, P. J., Boutelle, M. G., Hopwood, S. E., and Dunn, A. K. (2006). Evaluation of laser speckle flowmetry for imaging cortical perfusion in experimental stroke studies: quantitation of perfusion and detection of peri-infarct depolarisations. *J. Cereb. Blood Flow Metab.* 26, 645–653.

Williams, J. A., Imamura, M., and Fregni, F. (2009). Updates on the use of non-invasive brain stimulation in physical and rehabilitation medicine. *J. Rehabil. Med.* 41, 305–311.

Yanamoto, H., Nagata, I., Nakahara, I., Tohnai, N., Zhang, Z., and Kikuchi, H. (1999). Combination of intraischemic and postischemic hypothermia provides potent and persistent neuroprotection against temporary focal ischemia in rats. *Stroke* 30, 2720–2726.

Zakharov, P., Volker, A., Buck, A., Weber, B., and Scheffold, F. (2006). Quantitative modeling of laser speckle imaging. *Opt. Lett.* 31, 3465–3467.

Zakharov, P., Volker, A. C., Wyss, M. T., Haiss, F., Calcinaghi, N., Zunzunegui, C., Buck, A., Scheffold, F., and Weber, B. (2009). Dynamic laser speckle imaging of cerebral blood flow. *Opt. Express* 17, 13904–13917.

Zhou, C., Shimazu, T., Durduran, T., Luckl, J., Kimberg, D. Y., Yu, G., Chen, X. H., Detre, J. A., Yodh, A. G., and Greenberg, J. H. (2008). Acute functional recovery of cerebral blood flow after forebrain ischemia in rat. *J. Cereb. Blood Flow Metab.* 28, 1275–1284.

Conflict of Interest Statement: The authors declare that the research was conducted in the absence of any commercial or financial relationships that could be construed as a potential conflict of interest.

Received: 23 February 2010; paper pending published: 30 March 2010; accepted: 05 July 2010; published online: 30 July 2010.

Citation: Luckl J, Baker W, Sun Z-H, Durduran T, Yodh AG and Greenberg JH (2010) The biological effect of contralateral forepaw stimulation in rat focal cerebral ischemia: a multispectral optical imaging study. Front. Neuroenerg. ***2****:19. doi: 10.3389/fnene.2010.00019*